

# Application of Machine Learning to Predict the Dimensionless Bearing Capacity of Circular Footing on Layered Sand under Inclined Loads

Surya Pratap Singh\* and Amrit Kumar Roy

Department of Civil Engineering, NIT Hamirpur, Himachal Pradesh 177 005, India

Received: 28 March 2023; Accepted 23 May 2023

The present study aims to utilise machine learning techniques in order to predict the dimensionless bearing capacity ( $DBC_p$ ) of the circular footing on layered sand under inclined loading. For this objective, 2400 data points were collected from the literature using the finite element approach for the circular footing on layered sand under inclined loads. The dimensional bearing capacity ( $DBC_p$ ) was predicted using the independent variables thickness ratio ( $H/D$ ), load inclination angle ( $\alpha_1/90^\circ$ ), unit weight ratio of the loose sand layer to the dense sand layer ( $\gamma_2/\gamma_1$ ), friction angle ratio of the loose sand layer to the dense sand layer ( $\phi_2/\phi_1$ ), and embedment ratio ( $u/D$ ). Moreover, sensitivity analysis was performed to evaluate the effect of each independent variable on the structural integrity. At embedment ratios of 0, 1, and 2, the results show that load inclination is the primary factor influencing bearing capacity. In the end, six statistical parameters were used to evaluate the effectiveness of the machine learning model that had been built. For predicting the dimensionless bearing capacity of the circular footing on layered sand under inclined loading, the created model was found to work satisfactorily.

**Keyword:** Dimensionless bearing capacity, Machine learning techniques, Circular footing, Inclined loading

## 1 Introduction

The footing transfers the load of the structure to the ground below. The ratio of depth to width indicates whether a footing is shallow or deep. The load must be carried beneath the footing without settling or shearing. The ultimate bearing capacity of strip, circular, square, and rectangular footings on single-layer or layered soils has been determined via experimental, computational, and analytical research employing vertical and inclined loading<sup>1,2</sup>.

Several experimental methods, limit equilibrium approaches, and finite element analyses for assessing the bearing capacity of the strip footing on layered soils under vertical loading were compared. The authors concluded that the ratio of the thickness of the first layer to the thickness of the base and the loading condition were decisive and had a higher effect than the other variables evaluated<sup>3,4,5</sup>. Literature indicates that there is no ultimate bearing capacity equation for circular footings on layered sand under inclined loads. Expensive and time-consuming experimental or numerical studies are the only options to assess the bearing capacity in such situations. Calibrating and fitting the experimental or numerical data to develop a mathematical model to explain the relationships

between the multiple variables is another approach. Due to their potential to collect, analyze, and describe the dynamic interaction between a large numbers of variables without any prior knowledge of their bearing capacity, machine learning approaches are a superior option for modelling<sup>6,7,8</sup>.

Several machine learning algorithms (generalised reduced gradient, genetic programming, artificial neural networks, and evolutionary polynomial regression) were utilised to forecast the bearing capacity of a circular footing resting on layered soil under loading<sup>9,10</sup>. The study found that artificial neural networks performed better than previous methods (generalized reduced gradient, genetic programming, and evolutionary polynomial regression). The ultimate bearing capacity of circular footing on multilayered soil under vertical loading was predicted by<sup>11,12</sup> utilising an artificial neural network with certain metaheuristic techniques, including the dragonfly approach, Harris hawk's optimization, and sparse polynomial chaos expansions. Using elephant herding optimization, the shuffling frog leaping algorithm, the salp swarm algorithm, wind-driven optimization, and an artificial neural network to generate neural ensembles. The researcher studied the use of combining a black hole algorithm and a multi-verse optimizer with an artificial neural network (ANN) to

\*Corresponding author (E-mail: surya\_phdce@nith.ac.in)

create hybrid models; the black hole algorithm and multi-verse optimizer (MVO) can increase the accuracy of the artificial neural network. Also, the author claimed that MVO-ANN is a reliable method for the accurate estimation of bearing capacity<sup>13,14,15</sup>.

The shear strength was predicted using the salp swarm algorithm in<sup>16</sup> and the authors concluded that it may serve as a feasible alternative to conventional methods.<sup>17</sup> utilised multi-layer perceptron (MLP), Gaussian process regression multiple linear regression, simple linear regression, and support vector regression to forecast the factor of safety against slope failures<sup>18 19 20 21</sup>. The authors determined that the MLP outperformed previous models based on machine learning. According to the available literature, the novelty of this work lies in the fact that no previous work has used machine learning to forecast the bearing capacity of circular footings placed on layered sand under vertical and inclined loading. This research suggests using machine learning to predict the bearing capacity of an inclined circular foundation placed on layered sand. In addition, the majority of previous research on circular footings on layered sand subjected to vertical and inclined loading utilised experimental or numerical methods. Experimentally or numerically, the effect of embedment ratio on the bearing capacity of a circular footing on layered sand under an inclined surface has not been investigated.

The following objectives were considered throughout the development of this model:

- To identify the characteristics that influence the bearing capacity of the circular footing on layered sand under an inclined load, as well as the relationships between these parameters.
- To create a machine learning model for predicting bearing capacity and use statistical parameters to Testing the model's accuracy.
- To conduct sensitivity analysis in order to determine the effect of various parameters on output bearing capacity.
- To develop an empirical model applying machine learning technique to forecast the dimensionless bearing capacity of a circular footing lay on layered sand and subjected to vertical and inclined loading.

Figure 1 depicts the machine learning approach's design. As input variables, the footing embedment ratio ( $u/D$ ), upper dense sand layer thickness ratio ( $H/D$ ), unit weight ratio ( $\gamma_2/\gamma_1$ ) and friction angle

ratio ( $\phi_2/\phi_1$ ) load inclination ( $\alpha_1/90^\circ$ ) were all used to predict the output dimensionless bearing capacity.

## 2 Material and Methods

ANNs typically consist of a sequence of nodes grouped into three major levels: an input layer, one or more hidden layers, and an output layer. The development of an ANN model is described in depth<sup>22</sup>. The back propagation (BP) algorithm consists of layered connections (input, hidden and output). The output of the neuron or node in the input layer was supplied as an input to a node in the hidden layer, and the output of the neuron or node in the hidden layer was finally transmitted to the output layer. The problem at hand determines the number of hidden layers and the number

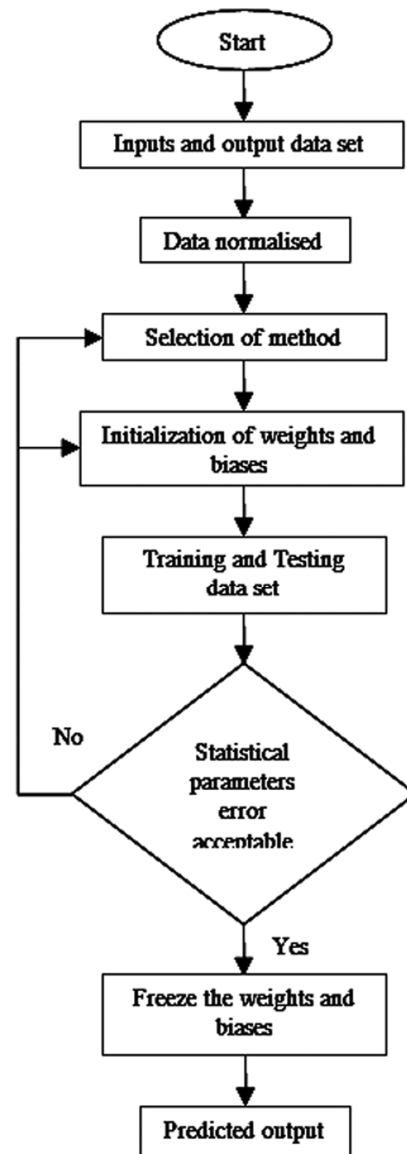


Fig. 1 — Illustration of a simplified machine learning approach.

of hidden layers. Hence, researchers were forced to rely on a time-consuming trial-and-error approach. Except for the input layer, each node in the BP network featured an activation function and a bias node. An input constant is incorporated in the bias. The activation function filters the aggregated result. Depending on the purpose, activation functions were utilised within ANN. The output layer computed output vectors corresponding to the solution of the problem. Input/output data were frequently represented as vectors (named as training pairs). The procedure is continued until the network error reaches a threshold, which is set by an error function (RMSE, root mean square error). Using the same method, the hidden and output layers were connected. During the network's training, the above technique was also utilised (input to the hidden and hidden to the output layer). Iteration refers to a single stage in the training sequence as a whole. Hence, the number of iterations is increased until the desired output is obtained (error is within the specified limit). ANN is a more trustworthy and accurate alternative to regression-

based approaches and formulas. This is because there is no formal expression between input and output variables in this modelling technique. A lengthy trial-and-error method is necessary for ANN to detect network features such as hidden layers and neurons.

### 2.1 Data-Set

In order to assess the dimensionless bearing capacity of a circular footing on layered sand (dense sand over loose sand) under inclined loading, 2400 data were collected using the Plaxis-3D software. Furthermore, none of these 2400 data has ever been reported in a study on machine learning. The data collected by the numerical analysis mentioned in [5-10] were utilised in the modelling. Table 1 contains further information regarding the employed parameters. Further numerical studies were conducted using the parameters indicated in Table 1 for various embedment ratios.

This study includes five input ( $\varphi_2/\varphi_1$ ,  $\gamma_2/\gamma_1$ , H/D, u/D,  $\alpha_1/90^\circ$ ) and one output (DBC<sub>p</sub>) variable for model development. Table 2 displays the minimum,

Table 1 — Range of parameters used for generating the data set for machine learning.

Parameters	Range of value				
Dense sand friction angles, ( $\varphi_1$ ) (Deg.)	41°	42°	43°	44°	45°
Loose sand friction angles, ( $\varphi_2$ ) (Deg.)	31°	32°	33°	34°	35°
Dense sand unit weight, ( $\gamma_1$ )	19.5	20	20.5	21	21.5
Loose sand unit weight, ( $\gamma_2$ )	14.5	15	15.5	16	16.5
Dense sand young's modulus, ( $E_1$ ) (MPa)	68.4	74.4	82.8	91.2	102.0
Loose sand Sand young's modulus, ( $E_2$ ) (MPa)	22.8	26.4	31.2	33.6	38.4
Dense sand dilation angle, ( $\psi_1$ ) (Deg.)	11°	12°	13°	14°	15°
Loose sand dilation angle, ( $\psi_2$ ) (Deg.)	1°	2°	3°	4°	5°
Thickness ratio, (H/D)	0.5	1.0	1.5	2.0	-
Embedded depth ratio, (u/D)	0	1.0	2.0	-	-
Load inclination, ( $\alpha_1$ ) (Deg.)	0°	10°	20°	30°	-

Table 2 — Data set used for training and Testing at various embedding ratios.

Input and output parameters	Embedded depth ratio, (u/D)	Training data set				Testing data set			
		Minimum	Maximum	Mean	Standard Deviation	Minimum	Maximum	Mean	Standard Deviation
$\varphi_2/\varphi_1$	u/D=0	0.69	0.85	0.775	0.041	0.69	0.85	0.775	0.041
$\gamma_2/\gamma_1$		0.67	0.85	0.764	0.043	0.67	0.85	0.764	0.043
H/D		0.5	2.0	1.248	0.559	0.5	2.0	1.248	0.559
$\alpha_1/90^\circ$		0	0.33	0.163	0.123	0	0.33	0.163	0.123
DBC <sub>A</sub>		5.28	170.49	48.723	35.632	6.30	176.50	53.839	39.520
$\varphi_2/\varphi_1$	u/D=1	0.69	0.85	0.775	0.041	0.69	0.85	0.775	0.041
$\gamma_2/\gamma_1$		0.67	0.85	0.764	0.043	0.67	0.85	0.764	0.043
H/D		0.5	2.0	1.248	0.559	0.5	2.0	1.248	0.559
$\alpha_1/90^\circ$		0	0.33	0.163	0.123	0	0.33	0.163	0.123
DBC <sub>A</sub>		22.01	403.15	124.20	79.652	26.80	425.30	142.10	91.696
$\varphi_2/\varphi_1$	u/D=2	0.69	0.85	0.775	0.041	0.69	0.85	0.775	0.041
$\gamma_2/\gamma_1$		0.67	0.85	0.764	0.043	0.67	0.85	0.764	0.043
H/D		0.5	2.0	1.248	0.559	0.5	2.0	1.248	0.559
$\alpha_1/90^\circ$		0	0.33	0.163	0.123	0	0.33	0.163	0.123
DBC <sub>A</sub>		38.51	562.34	184.19	111.591	48	610.1	213.33	130.86

Table 2 — Data set used for training and Testing at various embedding ratios.

Input and output parameters	Embedded depth ratio, (u/D)	Training data set				Testing data set			
		Minimum	Maximum	Mean	Standard Deviation	Minimum	Maximum	Mean	Standard Deviation
$\phi_2/\phi_1$	u/D=0	0.69	0.85	0.775	0.041	0.69	0.85	0.775	0.041
$\gamma_2/\gamma_1$		0.67	0.85	0.764	0.043	0.67	0.85	0.764	0.043
H/D		0.5	2.0	1.248	0.559	0.5	2.0	1.248	0.559
$\alpha_1/90^\circ$		0	0.33	0.163	0.123	0	0.33	0.163	0.123
DBC <sub>A</sub>		5.28	170.49	48.723	35.632	6.30	176.50	53.839	39.520
$\phi_2/\phi_1$	u/D=1	0.69	0.85	0.775	0.041	0.69	0.85	0.775	0.041
$\gamma_2/\gamma_1$		0.67	0.85	0.764	0.043	0.67	0.85	0.764	0.043
H/D		0.5	2.0	1.248	0.559	0.5	2.0	1.248	0.559
$\alpha_1/90^\circ$		0	0.33	0.163	0.123	0	0.33	0.163	0.123
DBC <sub>A</sub>		22.01	403.15	124.20	79.652	26.80	425.30	142.10	91.696
$\phi_2/\phi_1$	u/D=2	0.69	0.85	0.775	0.041	0.69	0.85	0.775	0.041
$\gamma_2/\gamma_1$		0.67	0.85	0.764	0.043	0.67	0.85	0.764	0.043
H/D		0.5	2.0	1.248	0.559	0.5	2.0	1.248	0.559
$\alpha_1/90^\circ$		0	0.33	0.163	0.123	0	0.33	0.163	0.123
DBC <sub>A</sub>		38.51	562.34	184.19	111.591	48	610.1	213.33	130.86

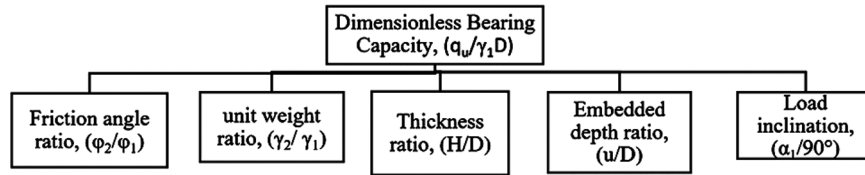


Fig. 2 — Independent variable to predict the dimensionless bearing capacity (output).

maximum, average, and standard deviation of all training and testing data at different embedment ratios. The data is divided 70/30 for training and testing at each embedment ratio. The thickness ratio (H/D), load inclination angle ( $\alpha_1/90^\circ$ ), unit weight ratio of the lower loose sand and upper dense sand ( $\gamma_2/\gamma_1$ ), friction angle ratio ( $\phi_2/\phi_1$ ), and embedment ratio all affect the circular footing's dimensionless bearing capacity (DBC<sub>A</sub>). Hence, a model was developed with all variables as inputs and the dimensionless bearing capacity (BCD<sub>p</sub>) as the output, defined in Equation (1).

$$BDC_p = \text{Input variable} \left( \frac{\phi_2}{\phi_1}, \frac{\gamma_2}{\gamma_1}, \frac{H}{D}, \frac{u}{D}, \frac{\alpha_1}{90^\circ} \right) = \text{Predicted Dimensionless bearing capacity for circular footing... (1)}$$

### 3 Results and Discussion

#### 3.1 Model Development

For the modelling, IBM SPSS Statistics was used. After training is complete, a set of connection weights and biases is formed. The mean square error (MSE) and the efficiency coefficient are significantly impacted by the number of input neurons in the hidden layer ( $R^2$ ). Figure 2 depicts the fluctuation of

both values as the number of neurons in the hidden layer increases. As observed, MSE decreases and  $R^2$  increases until the fifth neuron, after which a reversal occurs. Hence, the ideal neural network configuration of 4 inputs, 5 hidden neurons, and 1 output was chosen based on this investigation.

To validate the developed model's prediction accuracy, the model-obtained dimensionless bearing capacity (DBC<sub>p</sub>) was compared to the actual dimensionless bearing capacity (DBC<sub>A</sub>). Equations (2) to (7) describe the model's equations for measuring characteristics such as the correlation coefficient (r), the coefficient of determination ( $R^2$ ), the mean square error (MSE), the root mean square error (RMSE), the mean absolute error (MAE), and the mean absolute percentage error (MAPE).

Correlation coefficient (r)

$$r = \frac{\sum_{i=1}^n (DBC_A * DBC_p - \overline{DBC_A} * \overline{DBC_p})}{(n-1)S_A * S_p} \quad \dots (2)$$

Coefficient of determination

$$(R^2) R^2 = 1 - \frac{\sum_{i=1}^n (DBC_A - DBC_p)^2}{\sum_{i=1}^n (DBC_A - \overline{DBC_A})^2} \quad \dots (3)$$

Mean square error (MSE)

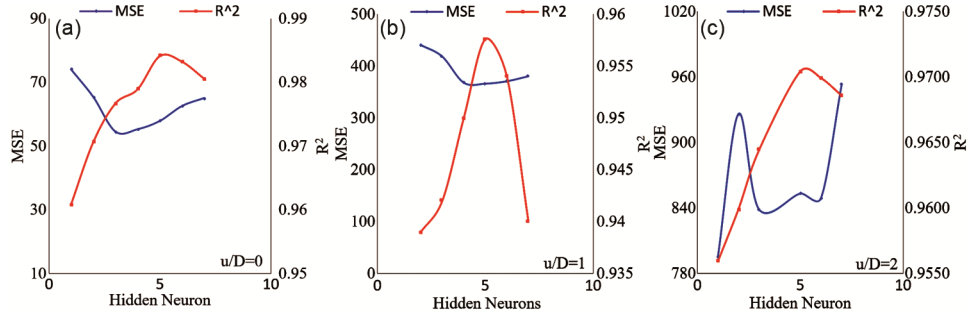


Fig. 3 — Estimation of the optimal number of neurons in the hidden layer at various embedding ratios.

Table 3 — Evaluating parameters for the proposed model at various embedding ratios.

Parameters	Embedded depth ratio, (u/D)	Training	Testing
r	u/D=0	0.9919	0.9851
R <sup>2</sup>		0.9840	0.9705
MSE		25.418	32.750
RMSE		5.042	5.645
MAE		3.438	3.508
MAPE (%)		11%	9%
r	u/D=1	0.9785	0.9698
R <sup>2</sup>		0.9576	0.9407
MSE		300.76	466.81
RMSE		17.31	21.54
MAE		12.15	14.71
MAPE (%)		12%	11%
r	u/D=2	0.9865	0.9820
R <sup>2</sup>		0.9733	0.9644
MSE		377.33	582.39
RMSE		19.41	24.08
MAE		14.26	15.81
MAPE (%)		10%	8%

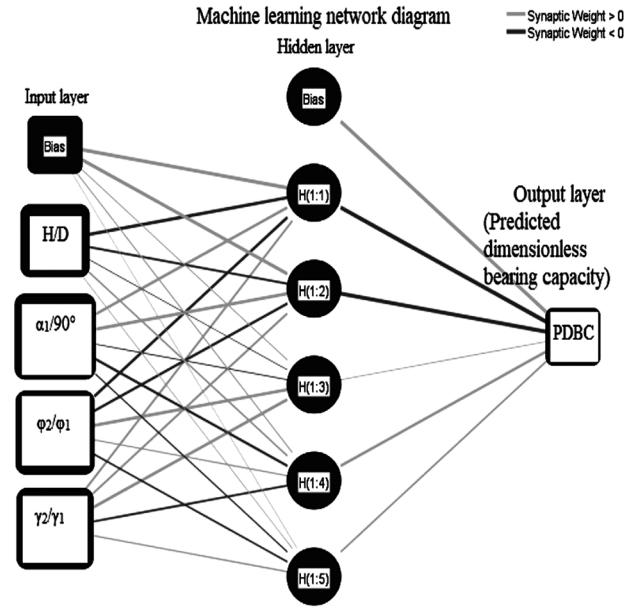


Fig. 4 — Network diagram of the model.

$$MSE = \frac{1}{n} \sum_{i=1}^n (DBC_A - DBC_P)^2 \quad \dots (4)$$

Root mean square error

$$(RMSE) \text{ RMSE} = \sqrt{\frac{1}{n} \sum_{i=1}^n (DBC_A - DBC_P)^2} \quad \dots (5)$$

Mean absolute error (MAE)

$$MAE = \frac{1}{n} \sum_{i=1}^n |DBC_A - DBC_P| \quad \dots (6)$$

Mean absolute percentage error

$$(MAPE) \text{ MAPE} = \left( \frac{1}{n} \sum_{i=1}^n |DBC_A - DBC_P| \right) * 100\% \quad \dots (7)$$

**Note:**  $DBC_A$ ,  $DBC_P$  represent actual and predicted bearing capacity, respectively,  $\overline{DBC_A}$ ,  $\overline{DBC_P}$  represent the mean of actual and expected bearing capacity, respectively.  $SD_A$ ,  $SD_P$  represent the standard deviation of actual and predicted bearing capacity, respectively.

Table 3 provides a summary of the assessment statistical parameters (r, R<sup>2</sup>, MSE, RMSE, MAE and MAPE) of the created model for both training and testing data. The coefficient of correlation (r) of the developed model was 0.9919, 0.9785, and 0.9865 for training data and 0.9851, 0.9698, and 0.9820 for testing data at embedding ratios of 0, 1, and 2. The correlation data coefficient represents the correlation and goodness-of-fit between the expected and actual values. |r| should range from 0.0 to 1.0. In actuality, the correlation must have a ‘r’ value between zero and one, which is a required but insufficient condition. In machine learning, only correlations that are near to one are acceptable. Table 3 provides additional evidence that all evaluative criteria are within accepted limits. Figure 3 illustrate the difference between the  $DBC_P$  computed by the neural network and the actual  $DBC_A$  for training and testing data, respectively. Figure 4 demonstrate that for both

training and testing data, the predicted and actual values of bearing capacity have coefficients of determination ( $R^2$ ) more than 0.95, showing that the model generated could be utilised to predict the output.

The connection weights between the input layer and the hidden layer, the weights between the hidden layer and the output layer, the bias at the input layer, and the bias at the output layer are represented by the matrices  $[x_{ji}]$ ,  $[y_{jk}]$ ,  $[z_j]$ , and  $[z_o]$ , respectively, once the model has been simulated under optimal conditions. In the matrices described below.

Generalized form of matrices

$$x_{ij} = \begin{bmatrix} x_{11} & x_{12} & x_{13} & x_{14} \\ x_{21} & x_{22} & x_{23} & x_{24} \\ x_{31} & x_{32} & x_{33} & x_{34} \\ x_{41} & x_{42} & x_{43} & x_{44} \\ x_{51} & x_{52} & x_{53} & x_{54} \end{bmatrix}, y_{jk} = \begin{bmatrix} y_{11} \\ y_{12} \\ y_{13} \\ y_{14} \\ y_{15} \end{bmatrix}, z_j = \begin{bmatrix} z_{11} \\ z_{12} \\ z_{13} \\ z_{14} \\ z_{15} \end{bmatrix}, z_o = [z_o] \quad \dots (8)$$

Where,  $x_{ij}$  represents the weight between the  $i^{th}$  neuron in the input layer and the  $j^{th}$  neuron in the hidden layer.

$y_{jk}$  represents the weight between the  $j^{th}$  neuron in the hidden layer and the  $k^{th}$  neuron in the output layer.  $z_j$  represents the bias at the  $j^{th}$  neuron in the hidden layer.

$z_o$  represents the bias at the output layer.

Matrices for  $u/D=0$ ,

$$x_{ij} = \begin{bmatrix} -0.489 & 0.662 & -0.030 & 0.005 \\ 0.685 & 0.493 & 0.151 & -0.161 \\ -0.226 & 0.502 & -0.070 & 0.071 \\ -0.108 & 0.389 & -0.311 & 0.479 \\ -0.281 & -0.030 & 0.130 & 0.325 \end{bmatrix}, y_{jk} = \begin{bmatrix} -1.901 \\ 0.609 \\ -1.049 \\ 0.209 \\ 0.067 \end{bmatrix}, z_i = \begin{bmatrix} 1.392 \\ 1.018 \\ -0.241 \\ 0.275 \\ 0.235 \end{bmatrix}, z_o = [0.799] \quad \dots (9)$$

Matrices for  $u/D=1$ ,

$$x_{ij} = \begin{bmatrix} 0.515 & -0.636 & -0.211 & 0.178 \\ 0.156 & 0.435 & 0.144 & -0.058 \\ 0.670 & -0.014 & 0.298 & -0.280 \\ -0.160 & -0.303 & 0.113 & 0.065 \\ 0.324 & 0.189 & 0.498 & 0.072 \end{bmatrix}, y_{jk} = \begin{bmatrix} 1.946 \\ -0.656 \\ 0.742 \\ 0.355 \\ 0.057 \end{bmatrix}, z_j = \begin{bmatrix} -1.312 \\ -0.586 \\ 0.595 \\ 0.280 \\ 0.477 \end{bmatrix}, z_o = [0.708] \quad \dots (10)$$

Matrices for  $u/D=2$ ,

$$x_{ij} = \begin{bmatrix} 0.397 & 0.547 & 0.01 & 0.076 \\ -0.354 & 0.385 & -0.106 & 0.038 \\ 0.418 & -0.776 & -0.011 & -0.074 \\ 0.515 & -0.019 & -0.157 & 0.228 \\ 0.415 & 0.1 & 0.324 & -0.386 \end{bmatrix}, y_{jk} = \begin{bmatrix} -0.527 \\ -0.995 \\ 1.481 \\ 0.489 \\ -0.010 \end{bmatrix}, z_j = \begin{bmatrix} -0.609 \\ 0.371 \\ -1.646 \\ 0.382 \\ -0.159 \end{bmatrix}, z_o = [1.119] \quad \dots (11)$$

**3.2 Sensitivity Analysis**

This section of the research evaluates the impact of various parameters on output dimensionless bearing capacity using sensitivity analysis. Based on the weight configuration, a sensitivity analysis was conducted using a method provided in <sup>23</sup> and employing the method stated therein. This method has drawbacks, however, due to the fact that it calculates the value of absolute weights. According to <sup>24</sup>, another way was used to sidestep this issue, and this method was utilised for the sensitivity analysis. This technique estimates, for each input neuron, the sum of the finalised connection weights from the input layer to the hidden layer neurons and from the hidden layer to the output layer neurons. Equation (12) is used to determine the individual contribution of each variable to a given input.

$$IR_j = \sum_{k=1}^h x_{jk} * x_k \quad \dots (12)$$

where  $x_{jk}$  represents the weight of the connection between the  $k^{th}$  neuron in the hidden layer and the  $j^{th}$  input variable.  $x_k$  represents the weight of the connection between a single output neuron and the  $k^{th}$  neuron of a hidden layer.  $IR_j$  represents significance relative to the  $j^{th}$  neuron in the input layer  $h$  represents the number of neurons in the hidden layer. Figure 5 illustrate the proportionate impact of each input variable on the output bearing capacity using equation (12).

Figure 6 analysis demonstrates that the output dimensionless bearing capacity was most affected by load inclination ( $\alpha_1/90^\circ$ ) for embedment ratios of 0, 1, and 2, i.e., 39%, 45%, and 44%, respectively. The difference between the most influential input factors  $H/D$  and  $\alpha_1/90^\circ$  is 0.05% 10% and 17% for an embedment ratio of 0,1 and 2 hence load inclination to output dimensionless bearing capacity is the most influential input variable. This may be due to the fact that when the load inclination increases; the horizontal displacement of the footing also increases,

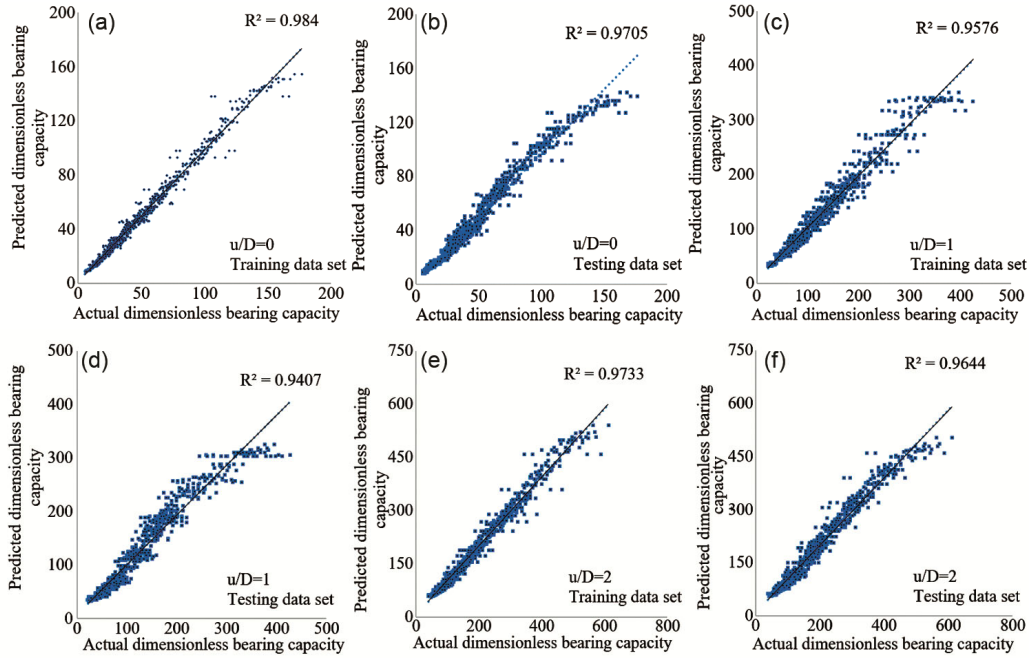


Fig. 5 — Comparison of predicted bearing capacity with the actual bearing capacity for (a) training data set for  $u/D = 0$ , (b). Testing data set for  $u/D = 0$ , (c) training data set for  $u/D = 1$ , (d) testing data set for  $u/D = 1$ , (e) training data set for  $u/D = 2$ , & (f) testing data set for  $u/D = 2$ .

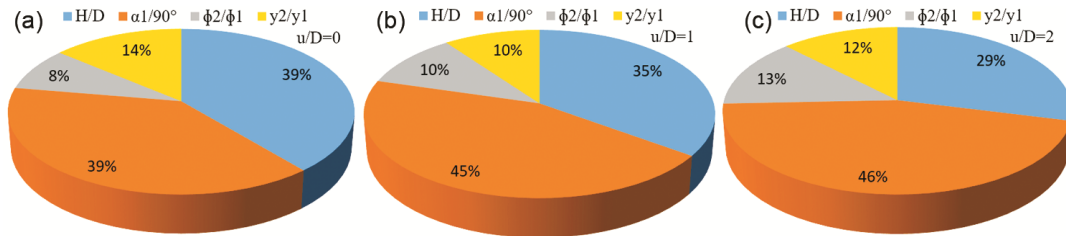


Fig. 6 — Analysis of the effect of each variable on the output's dimensionless bearing capacity for (a) embedded depth  $u/D = 0$ , (b) embedded depth ratio  $u/D = 1$ , & (c) embedded ratio  $u/D = 2$ .

causing the circular footing to fail. Hence, at all embedment ratios, the load inclination has the greatest impact on the output bearing capacity. Other input variables influenced the result in the following order:  $\alpha_1/90^\circ \geq H/D > \gamma_2/\gamma_1 > \phi_2/\phi_1$ ,  $\alpha_1/90^\circ > H/D > \gamma_2/\gamma_1 \geq \phi_2/\phi_1$ , and  $\alpha_1/90^\circ > H/D > \phi_2/\phi_1 > \gamma_2/\gamma_1$  for embedment ratios 0, 1, and 2, respectively. Likewise, as the thickness of the upper layer of dense soil increases, so does the dimensionless bearing capacity, and as the depth of the footing from the top surface of the upper dense soil increases, so does the surcharge load and, consequently, the dimensionless bearing capacity. The output is also affected by the properties of the overlying dense soil, since denser sand has better grain-to-grain interlocking than loose sand. Consequently, it can be concluded that sensitivity analysis is an effective method for properly connecting the input variables with the output dimensionless bearing capacity.

### 3.3 Formulation of the ANN model equation

As model parameters, the weights generated from the trained neural network are used to develop a model equation<sup>25</sup>. When considering the weights and biases specified by Equations (9) through (11), the ANN model equation has the following form:

$$DBC_p = [DBC_A]_{\{H/D, \alpha_1/90^\circ, \phi_2/\phi_1, \gamma_2/\gamma_1\}} = \text{fn}[z_o + \sum_{i=1}^h \{y_{ij} \text{fn}(\sum_{j=1}^n x_{ij} S_i)\}]$$

Here,

fn= Sigmoid activation function

$z_o$ = Output bias

$h$ = hidden number of neuron

$y_{jk}$ = Output weights

$n$ = number of input variable

$x_{ij}$ = input weights

$S_i$ = normalised inputs

Generalised equation of sigmoid activation function,

Linear programming,

$$A_{ii} = x_{i1} * \left(\frac{H}{D}\right) + x_{i2} * \left(\frac{\alpha_1}{90^\circ}\right) + x_{i3} * \left(\frac{\varphi_2}{\varphi_1}\right) + x_{i4} * \left(\frac{\gamma_2}{\gamma_1}\right) \dots (13)$$

Non-Linear programming,

$$B_{jj} = \left(\frac{y_{jk}}{1+e^{-A_{ii}}}\right) \dots (14)$$

$$DBC_P = \sum_{i=0}^n (B_{jj}) + z_0 \dots (15)$$

$$B_{11} = \left(\frac{y_{11}}{1+e^{-A_{11}}}\right) \dots (21)$$

$$B_{12} = \left(\frac{y_{12}}{1+e^{-A_{12}}}\right) \dots (22)$$

$$B_{13} = \left(\frac{y_{13}}{1+e^{-A_{13}}}\right) \dots (23)$$

$$B_{14} = \left(\frac{y_{14}}{1+e^{-A_{14}}}\right) \dots (24)$$

$$B_{15} = \left(\frac{y_{15}}{1+e^{-A_{15}}}\right) \dots (25)$$

Model equation development requires the determination of parameters  $A_{11}$ – $A_{15}$  and  $B_{11}$ – $B_{15}$  via Equations (16-20) and (21-25), respectively.

$$A_{11} = x_{11} * \left(\frac{H}{D}\right) + x_{12} * \left(\frac{\alpha_1}{90^\circ}\right) + x_{13} * \left(\frac{\varphi_2}{\varphi_1}\right) + x_{14} * \left(\frac{\gamma_2}{\gamma_1}\right) + z_{11} \dots (16)$$

$$A_{12} = x_{21} * \left(\frac{H}{D}\right) + x_{22} * \left(\frac{\alpha_1}{90^\circ}\right) + x_{23} * \left(\frac{\varphi_2}{\varphi_1}\right) + x_{24} * \left(\frac{\gamma_2}{\gamma_1}\right) + z_{12} \dots (17)$$

$$A_{13} = x_{31} * \left(\frac{H}{D}\right) + x_{32} * \left(\frac{\alpha_1}{90^\circ}\right) + x_{33} * \left(\frac{\varphi_2}{\varphi_1}\right) + x_{34} * \left(\frac{\gamma_2}{\gamma_1}\right) + z_{13} \dots (18)$$

$$A_{14} = x_{41} * \left(\frac{H}{D}\right) + x_{42} * \left(\frac{\alpha_1}{90^\circ}\right) + x_{43} * \left(\frac{\varphi_2}{\varphi_1}\right) + x_{44} * \left(\frac{\gamma_2}{\gamma_1}\right) + z_{14} \dots (19)$$

$$A_{15} = x_{51} * \left(\frac{H}{D}\right) + x_{52} * \left(\frac{\alpha_1}{90^\circ}\right) + x_{53} * \left(\frac{\varphi_2}{\varphi_1}\right) + x_{54} * \left(\frac{\gamma_2}{\gamma_1}\right) + z_{15} \dots (20)$$

$$DBC_P = B_{11} + B_{12} + B_{13} + B_{14} + B_{15} + z_0 \dots (26)$$

Equation (26) represents the final expression, which is the normalised output. Equations (27-30) represent the output in the renormalized form of embedded footings 0, 1 and 2.

$$[DBC_A] = DBC_P = 0.5 * (DBC_P + 1) [(DBC_{P_{max}}) - (DBC_{P_{min}})] + (DBC_{P_{min}}) \dots (27)$$

$$[DBC_A] = DBC_{0P} = 0.5 * (DBC_P + 1) [171.225] + (5.275) \dots (28)$$

$$[DBC_A] = DBC_{1P} = 0.5 * (DBC_P + 1) [403.29] + (22.01) \dots (29)$$

$$[DBC_A] = DBC_{2P} = 0.5 * (DBC_P + 1) [571.593] + (38.507) \dots (30)$$

Embedment ratios of 0, 1, and 2 are proposed as the final model expressions in Equations (28), (29), and (30), respectively, based on data obtained per [5,13]. The dimensionless bearing capacity of the circular footing on the layered sand subject to inclined loading is calculated using the given formulae. Figures 7 present a comparison of the actual bearing capacity to the predicted bearing capacity derived from model Equations (28), (29), and (30). (30).

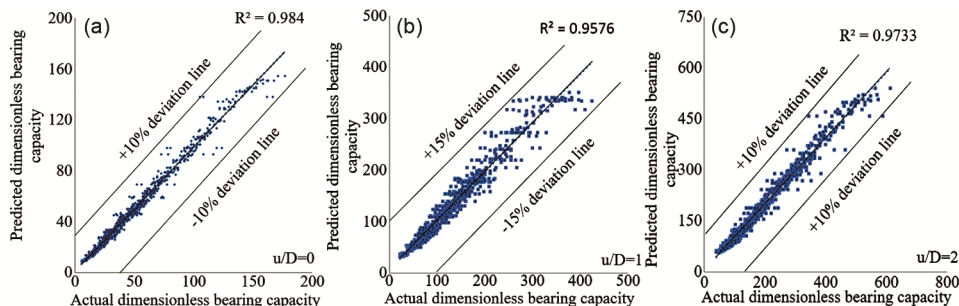


Fig. 7 — Comparison between the actual bearing capacity and the predicted bearing capacity using model equations at (a) embedded depth ratio  $u/D = 0$ , (b) embedded depth ratio  $u/D = 1$ , & (c) embedded depth ratio  $u/D = 2$ .

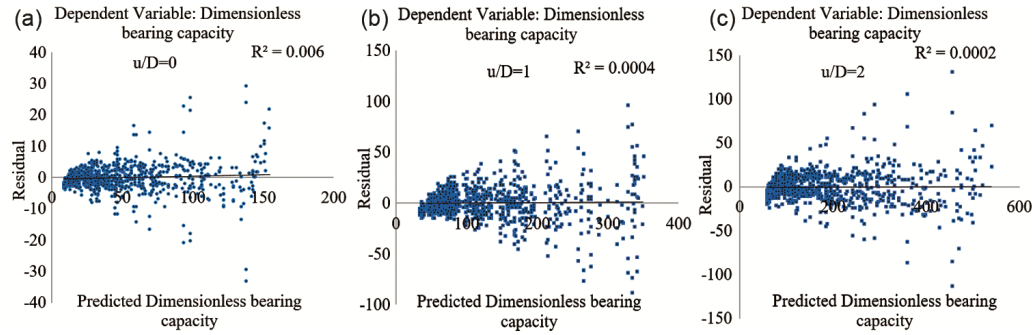


Fig. 8 — Residual by predicted chart using model equation at (a) embedded depth ratio  $u/D = 0$ , (b) embedded depth ratio  $u/D = 1$ , & (c) embedded depth ratio  $u/D = 2$ .

Table 4 — Comparison of the present study with the literature varying thickness ratio.

H/D	Present Study ( $\phi_1=45^\circ, \gamma_1=21.5 \text{ kN/m}^3$ and $\phi_2=34^\circ, \gamma_2=16 \text{ kN/m}^3$ )	Khatri et al (2021) ( $\phi_1=46^\circ, \gamma_1=22 \text{ kN/m}^3$ and $\phi_2=34^\circ, \gamma_2=16 \text{ kN/m}^3$ )		Hanna (1982) ( $\phi_1=47.7^\circ, \gamma_1=16.33 \text{ kN/m}^3$ and $\phi_2=34^\circ, \gamma_2=13.78 \text{ kN/m}^3$ )
		Lower Bound	Upper Bound	
0.5	46.05	34.41	39.50	36.75
1.0	70.16	90.76	95.35	61.23
1.5	112.10	109.47	116.32	94.95
2.0	150.59	156.73	162.83	141.87

Table 5 — Comparison of the present study with the literature varying load inclination.

H/D	$\alpha_1=0^\circ$		$\alpha_1=10^\circ$		$\alpha_1=20^\circ$		$\alpha_1=30^\circ$	
	Present Study	Meyerhof (1978)	Present Study	Meyerhof (1978)	Present Study	Meyerhof (1978)	Present Study	Meyerhof (1978)
0.5	106.47	67.65	69	54.51	41.81	37.56	26.94	21.25
1.0	177.24	107.11	108.67	81.64	65.69	60.71	35.32	38.16
1.5	255.09	165.28	167.43	123.12	103.28	91.07	54.16	63.31
2.0	322.67	235.04	220.69	185.01	144.79	134.86	70.91	88.46

Figures analysis shows that at embedment ratios of 0, 1, and 2, the predicted and actual dimensionless bearing capacities differed by 10%, 15%, and 10%, respectively. According to [35], the average permitted error rate for predictions in geotechnical engineering is 10%. Thus, the suggested models can accurately predict the dimensionless bearing capacity of circular footings resting on layered soils under inclined loading. The Fig. 8 illustrates the residual when predicting the dimensionless bearing capacity for different embedment ratios.

**3.4 Comparison**

The experimental results of <sup>2</sup> and the upper and lower bound theorems of <sup>26</sup> were compared to the results of the proposed model for both surface footings and embedded depth footings. It is important to note that <sup>2</sup> used friction angles of  $47.5^\circ$  and  $34^\circ$  and unit weights of  $13.78 \text{ kN/m}^3$  and  $16.33 \text{ kN/m}^3$ , respectively, for the upper dense sand layer and the bottom loose sand layer. <sup>26</sup> utilised the friction angle

and unit weight for the upper dense sand layer, which was  $46^\circ$  and  $22 \text{ kN/m}^3$ , and the lower sand layer, which was  $34^\circ$  and  $16 \text{ kN/m}^3$ . The comparison in Table 4 is based on the thickness ratio (H/D) of the surface footing. The average percentage of variance in the dimensionless bearing capacity between this study, <sup>2</sup> and <sup>26</sup> for surface footing is 11.23%, 6.80%, 8.28%, 2.98% and 7.66%, 15.22%, 1.85%, 3.91% for thickness ratios of 0.5, 1.0, 1.5, and 2.0.

The present research is compared to <sup>3</sup> for embedded footing ( $u/D = 1$ ) using thickness ratio (H/D) and load inclination (Table 5). According to the results, the average percentage of deviation in the dimensionless bearing capacity is minimum 3.55% for the lower thickness ratio ( $H/D = 2$ ) and load inclination ( $\alpha_1=20^\circ$ ), and it goes up to 22.29% for the upper thickness ratio ( $H/D = 0.5$ ) for the load inclination ( $\alpha_1=0^\circ$ ).

It's possible that every discrepancy results from the fact that <sup>3</sup> and <sup>2</sup> assumed that the load spread angle was the same as the angle of load inclination.

#### 4 Conclusion

Utilizing a method based on machine learning, this research aims to create model equations for the dimensionless bearing capacity of a circular footing placed on layered sand under the influence of inclined loading. The independent variables used to predict the output dimensionless bearing capacity were the thickness ratio ( $H/D$ ), load inclination angle ( $\alpha/90^\circ$ ), unit weight ratio of lower loose and upper dense sand layer ( $\gamma_2/\gamma_1$ ), friction angle ratio of lower loose and upper dense sand layer ( $\phi_2/\phi_1$ ), and embedment ratio ( $u/D$ ), with DBCP as the output. The following conclusions can be drawn from the above discussions:

- i For embedment ratios of 0, 1, and 2, the same sigmoid activation function is used to predict the output bearing capacity of a circular footing on layered sand under inclined loading.
- ii The sigmoid activation function is found to have optimal values for all evaluation metrics ( $r$ ,  $R^2$ , MSE, RMSE, MAE, and MAPE).
- iii With embedding ratios of 0, 1, and 2, the observed coefficients of determination for the training and testing data were 0.984, 0.957, and 0.973 and 0.97, 0.94, and 0.964, respectively.
- iv With embedment ratios of 0, 1, and 2, the mean absolute percent error on training and testing data is 11, 12, 10, and 9, 11, 8, respectively.
- v At embedment ratios of 0, 1, and 2, load inclination was the most important input variable in determining the dimensionless bearing capacity, with respective weights of 39%, 45%, and 46%.
- vi At embedment ratios of 0, 1, and 2, the actual and predicted dimensionless bearing capacities deviated by 10%, 15%, and 10%, respectively.
- vii For all embedded ratios of 0, 1, and 2, the computed error between predicted and actual dimensionless bearing capacity is 0.006, 0.0004, and 0.0002 respectively.

The major objective of this research was to determine how machine learning may be used to predict the dimensionally independent bearing capacity of a circular

footing resting on layered sand while subjected to inclined loading. Within the allowable variation, the given models reliably predict the dimensionally independent bearing capacity for a variation of embedment ratios. Also, this work's proposed formulas will help researchers avoid costly and time-consuming experiments or numerical simulations.

#### References

- 1 Kumar J, Chakraborty M & J Chakraborty, M Bear Capacit *Circ Found Layer sand -clay media Soils Found* 2015 55(5)1058.
- 2 HANNA, A M, *Can Geotech J V* 19, 392 (1982).
- 3 Meyerhof G G & Hanna A M, *Can Geotech J*, 15 (1978) 565.
- 4 Panwar V & Dutta R K, *J Achiev Mater Manuf Eng*, 108(2021) 49.
- 5 Singh S P & Roy A K, *Civ Environ Eng Reports*, 31(2021) 29.
- 6 Nikraz H & M A Bearing, *J Earth Sci Clim Change*, 06 (2015).
- 7 Singh S P & Roy A K, *J Min Environ*, 13(2022)1015.
- 8 Das P P & Khatri V N, *Civ Eng*, 84(2020) 203.
- 9 Trzepieciński T & Najm S M, *Materials (Basel)*. 15, (2022).
- 10 Kumar Singh A, 1(2022) doi:10.20944/preprints2022 06.0163.v1.
- 11 Nazir R, Momeni E, Marsono K & Maizir H, *J Teknol*, 72 (2015) 9.
- 12 Marto A, Hajihassani M & Momeni E, *Appl Mech Mater*, 567 (2014) 681.
- 13 Acharyya R, Dey A & Kumar B, *Int J Geotech Eng*, 14 (2020) 176.
- 14 Moayed H, Gör M, Kok Foong L & Bahiraci M, *J Int Meas Confed*, 172 (2021).
- 15 Moayed H, Bui D T & Ngo P T T, *Appl Sci*, 9 (2019).
- 16 Sasmal S K & Behera R N, *Int J Geotech Eng* 15 (2021) 834.
- 17 Gupta R, Goyal K & Yadav N, *Int J Geomech* 16 (2016) 1.
- 18 Bui D T, Moayed H, Gör M, Jaafari A & Foong L K ISPRS, *Int. J. Geo-Information* 8 (2019).
- 19 Sethy B P, Patra C, Das B M & Sobhan K *Int J Geotech Eng*, 15 (2021) 1252.
- 20 Behera R N, Patra C R, Sivakugan N & Das B M, *Int J Geotech Eng*, 7 (2013) 36.
- 21 Behera R N, Patra C R, Sivakugan N & Das B M, *Int J Geotech Eng*, 7 (2013) 165.
- 22 Shahin M A, Jaksa M B & Maier H R, *Aust Geomech J*, 36 (2001) 49.
- 23 Garson G D, *Artif Intell Exp*, 6 (1991) 47.
- 24 Olden J D & Jackson D A, *Ecol Modell*, 154 (2002) 135.
- 25 Goh A T C, Kulhawy F H & Chua C G, 31 (2005) 84.
- 26 Das P P, Khatri V N & Kumar J, *Arab J Geosci*, 15 (2022) 1.